

## Supporting Information for

# Structural, Magnetic and Optical Properties of a Fe<sup>III</sup> Dimer Bridged by the Meridional Planar Divergent *N,N'*-bis(salicyl)hydrazide and its Photo- and Electro-Chemistry in Solution

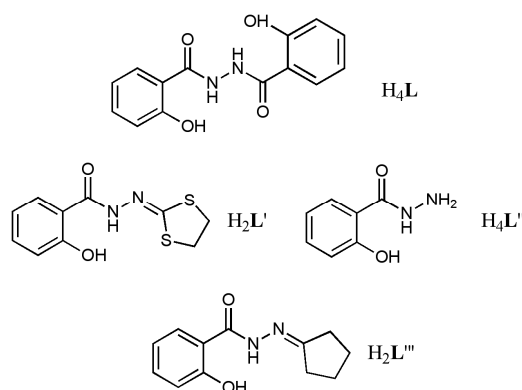
Khaled Cheaib,<sup>a</sup> David Martel,<sup>b</sup> Nicolas Clément,<sup>a</sup> Fabrice Eckes,<sup>a</sup> Stéphanie Kouaho,<sup>a</sup> Guillaume Rogez,<sup>c</sup> Samuel Dagherne,<sup>a</sup> Mohamedally Kurmoo<sup>a</sup>, Sylvie Choua<sup>d</sup> and Richard Welter\*,<sup>a</sup>

## Experimental

### Synthesis

**H<sub>2</sub>L'** and **H<sub>2</sub>L'''** were prepared using previously published procedures [1]. **H<sub>4</sub>L''** was obtained commercially (Acros Organics) and was used as received.

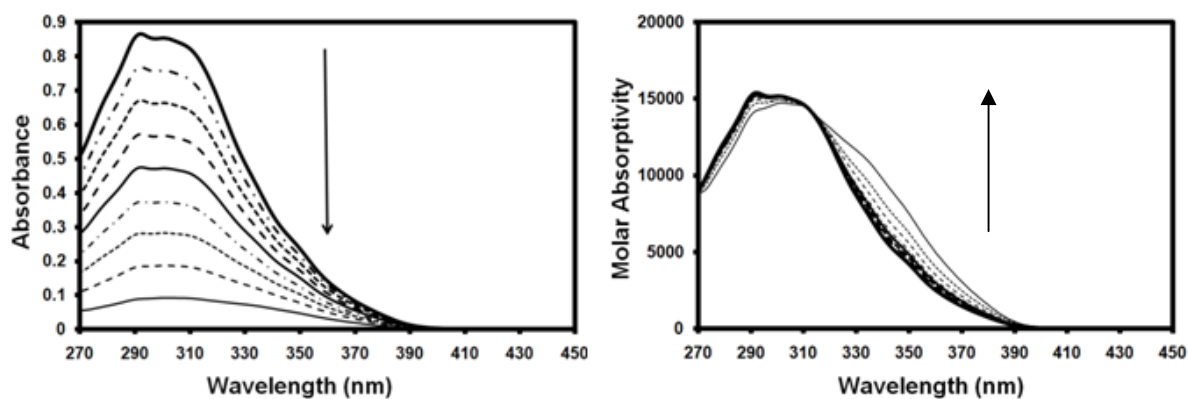
The studied molecules are depicted scheme SS1.



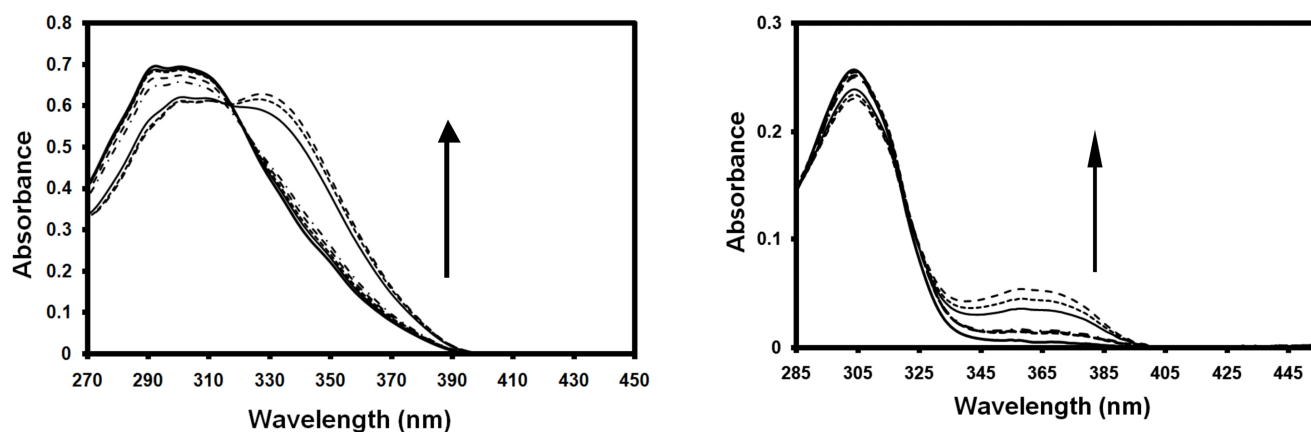
SS1: Molecules investigated in this work

### UV-Visible measurements

Similar behaviour as **H<sub>4</sub>L** is observed in the case of the compound **H<sub>2</sub>L'** for the evolution vs. the concentration (Figure S1), the addition of base (Figure S2) and acid (figure S3). Although the components of the measured absorption band are less well resolved (see later discussion).



**S1:** Absorption spectra (left) and molar absorptivity (right) of  $H_2L'$  for different concentrations:  $5.6 \cdot 10^{-5} M$ ,  $5.0 \cdot 10^{-5} M$ ,  $4.4 \cdot 10^{-5} M$ ,  $3.7 \cdot 10^{-5} M$ ,  $3.1 \cdot 10^{-5} M$ ,  $2.5 \cdot 10^{-5} M$ ,  $1.9 \cdot 10^{-5} M$ ,  $1.3 \cdot 10^{-5} M$  and  $6.3 \cdot 10^{-6} M$   
(The arrow indicates the sense of the absorbance changes with decrease of the concentration)

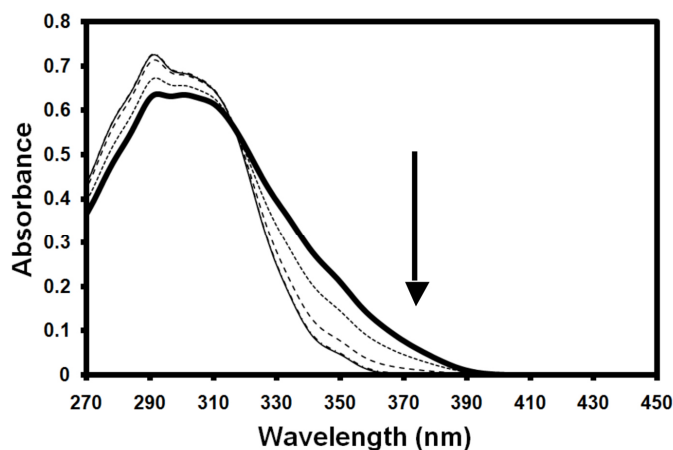


**S2:** Absorbance changes resulting from the addition of triethylamine

Left:  $H_2L'$  ( $5 \cdot 10^{-5} M$ ) with triethylamine concentrations equal to  $0 M$ ,  $5 \cdot 10^{-5} M$ ,  $1 \cdot 10^{-4} M$ ,  $2 \cdot 10^{-4} M$ ,  $3 \cdot 10^{-4} M$ ,  $5 \cdot 10^{-3} M$ ,  $1 \cdot 10^{-2} M$  and  $1.5 \cdot 10^{-2} M$

Right:  $H_4L''$  ( $5 \cdot 10^{-5} M$ ) with triethylamine concentrations equal to  $0 M$ ,  $5 \cdot 10^{-5} M$ ,  $1 \cdot 10^{-4} M$ ,  $1.5 \cdot 10^{-4} M$ ,  $6 \cdot 10^{-3} M$ ,  $1.8 \cdot 10^{-2} M$  and  $3.7 \cdot 10^{-2} M$

(The arrows indicate the sense of the absorbance changes due to addition of triethylamine)

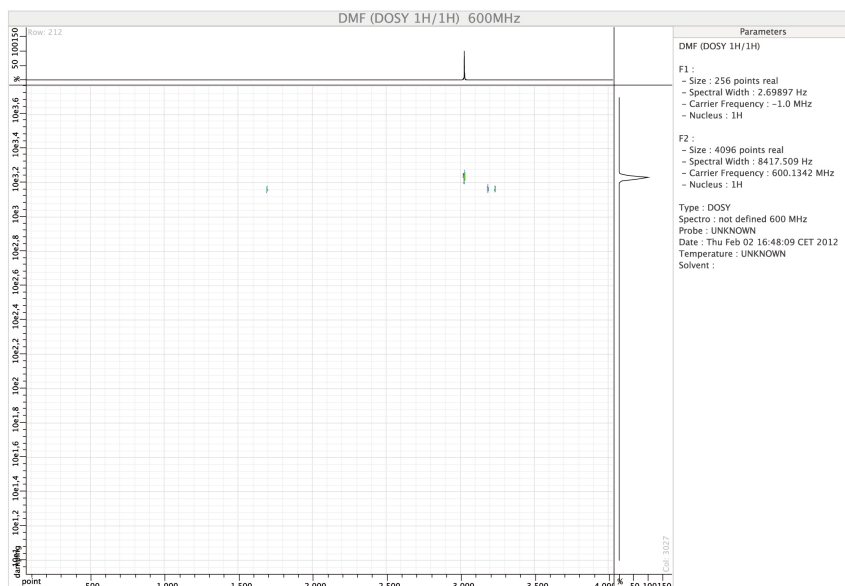


**S3:** Absorbance changes due to the addition of HCl

$H_2L'$  ( $5 \cdot 10^{-5} M$ ) with HCl concentrations of 0 M,  $5 \cdot 10^{-5} M$ ,  $1 \cdot 10^{-4} M$ ,  $1.5 \cdot 10^{-4} M$ ,  $2 \cdot 10^{-4} M$

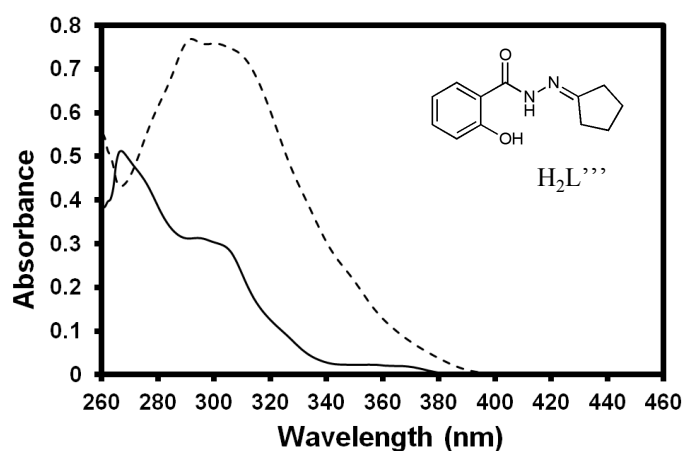
(The arrows indicate the sense of the absorbance changes due to addition of HCl)

These results indicate that the spectroscopic changes reflect the protonation states of the molecules. Each molecule possesses a phenol and hydrazide or hydrazone functions which can play the role of acid groups [2-4]. In the case of  $H_4L$ , aggregation phenomenon is excluded considering DOSY NMR measurement depicted on Figure S4 (see the text of the article for the hydrodynamic volume data).



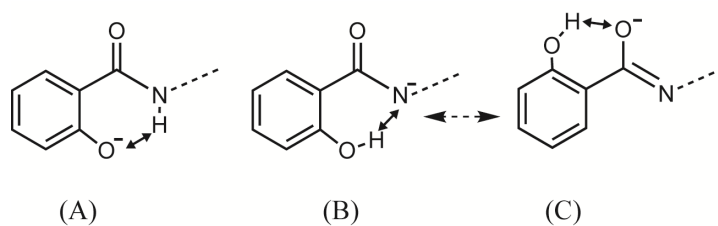
**S4:** DOSY-NMR of 1 mM  $H_4L$  in DMF

Thus, for both the present and previously studied systems [2,3], a basic understanding can be gained of their spectroscopic characteristics. In the selected wavelength range, electronic absorption spectra are a convolution of several transitions involving the functions Ph-OH, Ph-CO-NH-N=R and Ph-CO-NH-. The nature (electron donor or not) of R has a strong influence on their absorbance properties within the molecule and on the overlapping of signals. An example of spectral changes can be seen when the electron donor group of  $H_2L'$  is exchange by a group with lower electron donor character (Figure S5). Two bands are observed which can correspond to a splitting of the broad signal of  $H_2L'$  and can be assigned to transition involving the overall function  $R'-CO-NH-N=R$  [2, 3].



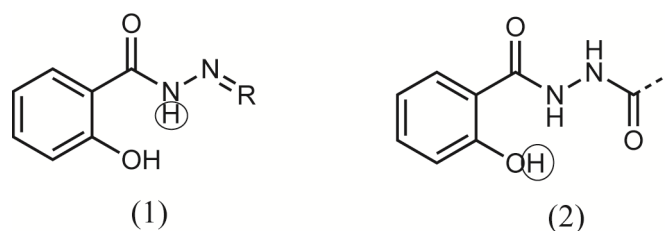
S5: Absorbance spectra of  $H_2L'$  (dotted line) and  $H_2L'''$  (thin line), both at  $5 \cdot 10^{-5} M$

Other transitions are present under the two broad bands. Indeed, the overall signal corresponds to the convolution involving the acid-base equilibria of the  $CO-NH-N=R \leftrightarrow CO-N^-N=R$  and  $Ph-OH \leftrightarrow Ph-O^-$ . For these reactions, intramolecular hydrogen bonding, which could influence the absorbance properties, have to be taken into account. From different studies [2,3], several types of hydrogen bonds could be considered as depicted on scheme SS2.



SS 2: Potential intramolecular hydrogen bonds occurring in studied (salicyl)hydrazine derivatives.

Focusing on these collected data, it is possible to underline two points: Firstly, for the same concentration, the second band occurring into  $H_4L$  spectrum is more prominent compared to the first one, than what is observed in the case of  $H_2L'$ . Secondly, with two equivalents of triethylamine, this second band develops more for  $H_4L$  compared to  $H_2L'$  or  $H_4L''$ . The origin of this behaviour could simply be attributed to the two equivalent acid functions present in the  $H_4L$  molecule. Thus, higher signal can be expected. But, a second hypothesis, based on the difference of the acidity power of the molecules, could also be pointed out. All the investigations performed in this study would be in agreement with the second approach (see discussion below and electrochemical section). In the case of  $H_2L'$ , the combination of the hydrazone and hydrazide function would confer a greater acidity to the N-H proton than this of  $H_4L$  (scheme SS3). This effect can be supported considering the electronic delocalizations effect which stabilize the  $N^-$  state [2,3]. In these conditions, this proton would be more acid in the case of  $H_2L'$ .



**SS 3:** The circle indicates the more acid proton in the case of:  
(1)  $H_2L'$  or  $H_4L''$  and (2)  $H_4L$

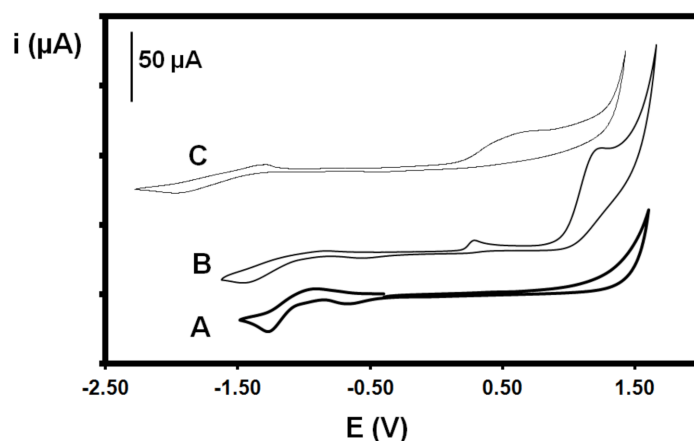
This last hypothesis would allow us to explain the observed results. In the case of  $H_2L'$ , some electronic transitions are related to the acid-base reaction involving the hydrazide/hydrazone part which often overlap with the  $Ph-OH/PhO^-$  group [2,3]. If the  $NH$  proton are acid and more than in the case of  $Ph-OH$ , then the molecule could be mainly in the case B and C of the scheme 2. In this context, the proportion of  $Ph-O^-$  is small. For  $H_4L$ , the opposite behaviour would be the origin of the observed property because of the lack of hydrazide/hydrazone part. The  $NH$  proton, which is less acid, leads the stabilisation of the  $Ph-O^-$  group and even increases the acidity of the phenol function. Then, the case A of the scheme 2 can exist and the proportion of  $Ph-O^-$  would be more important. One can notice that the enol equilibrium is not involved in the reasoning. Because it is common to all molecules, one can assume that it brings equivalent effect, therefore it is not a pertinent parameter.

When a base is added to a solution of  $H_2L'$ , the predominant reaction would be the exchange of the proton from  $NH$  function. More this process evolves and more  $Ph-OH$  would be involved via equilibrium and hydrogen bond. Then, only after removing a significant part of

NH protons, the Ph-OH protons would be affected. In the case of  $H_4L$ , less quantity of base will be necessary because the main protons source is the Ph-OH function. Regarding the addition of HCl acid, the difference between  $H_4L$  and  $H_2L'$  are lower than in the precedent case. In the case of addition of HCl acid, all the basic functions can react.  $H_2L'$  has three basic sites which are the  $N^- \leftrightarrow C-O^-$ ,  $Ph-O^-$  and a third which corresponds to the protonation of  $N=C$ . The electronic transition should again overlap with the other processes to form the broad band at short wavelengths. The molecule  $H_4L$  has both  $Ph-O^-$  and  $N^-$  functions then the necessary amount of acid should be higher for  $H_2L'$  than for  $H_4L$ .

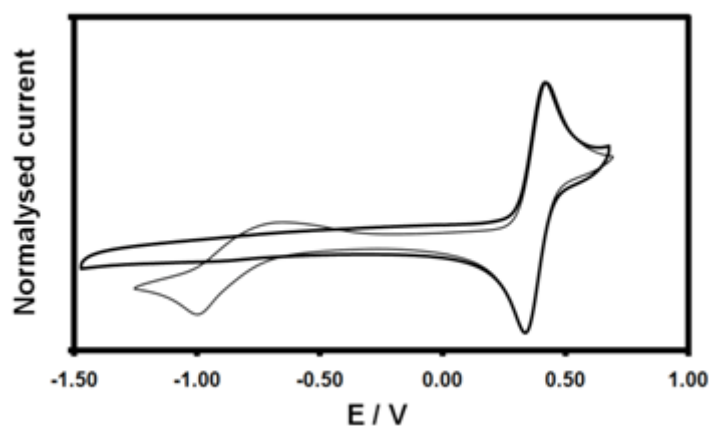
## Electrochemical measurements

Cyclic voltammograms for the compounds  $H_4L$ ,  $H_2L'$  and  $H_4L''$  are given in Figure S6. All show a quasi reversible reduction step but only  $H_2L'$  and  $H_4L''$  show oxidation processes (irreversible).



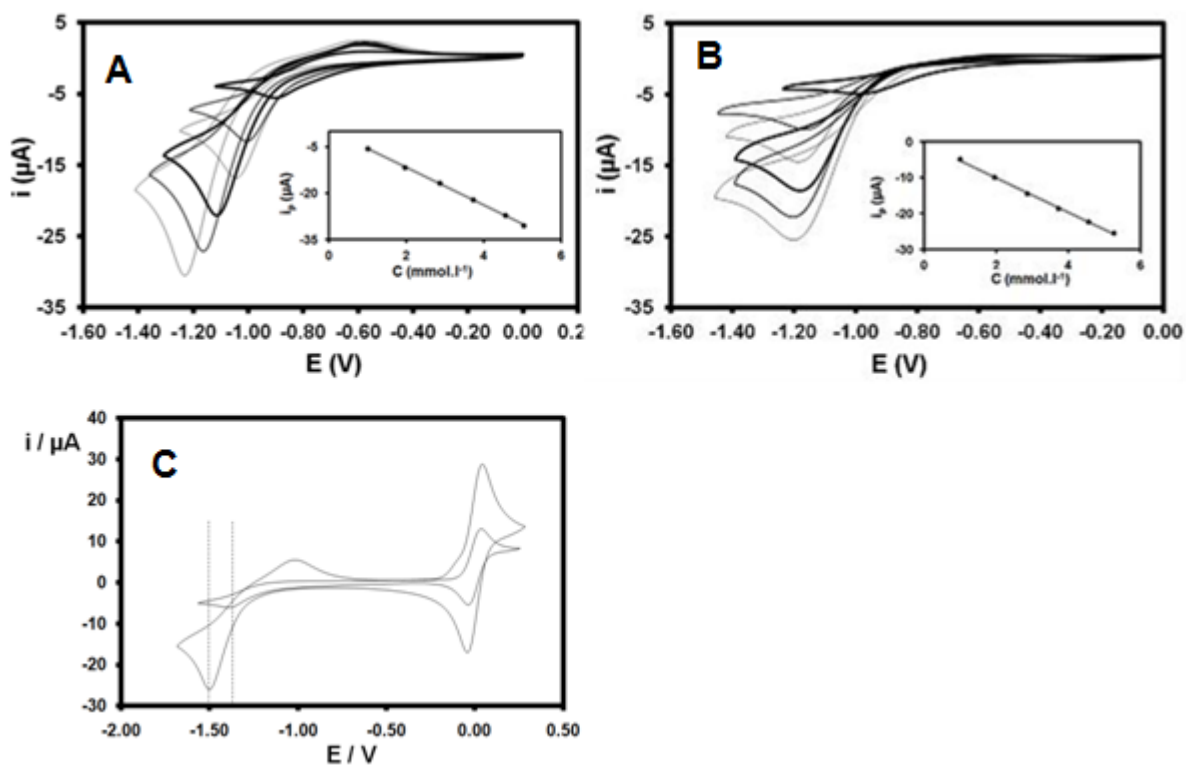
**S6:** Cyclic voltammograms of A)  $H_4L$ , B)  $H_2L'$  and C)  $H_4L''$ :  $C = 5mM$ , Pt working electrode, Pt pseudo reference electrode,  $TBAPF_6 = 150 mM$ ,  $v = 0.1 V.s^{-1}$

This behaviour is consistent with the electronic distribution on the hydrazone function which only occurs on molecules  $H_2L'$  and  $H_4L''$ . The reduction step corresponds to proton reduction as it can be deduced from a comparison involving carbon and platinum electrodes [5] (Figure S7).



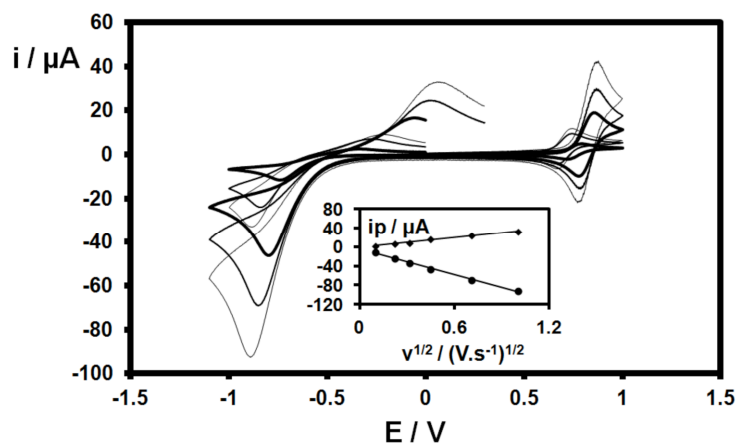
**S7:** Cyclic voltammograms of  $H_4L$  (5 mM) recorded with carbon (thick line) and platinum (thin line) electrodes. DMF,  $TBAPF_6 = 150$  mM,  $v = 0.1$  V.s<sup>-1</sup>.

Cyclic voltammetry as a function of concentration provided a satisfyingly linear current-concentration relation (Figure S8) for both  $H_4L$  and  $H_2L'$ .



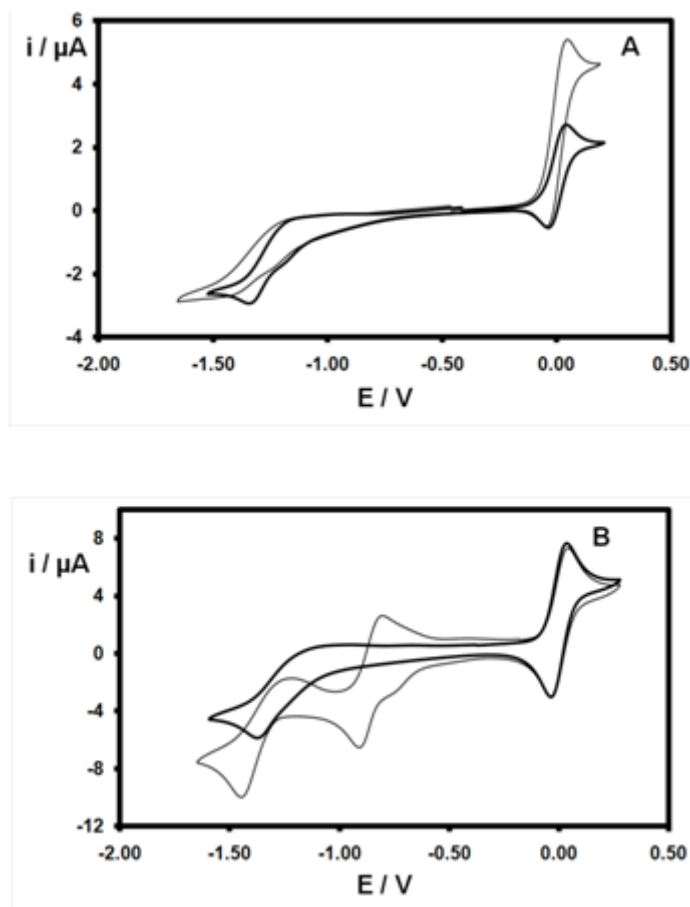
**S8:** Cyclic voltammograms of A)  $H_4L$  and B)  $H_2L'$  for different concentrations: 1, 1.95, 2.85, 3.72, 4.54 and 5 mM. C) Cyclic voltammogram of  $H_4L$  for 1 mM and 5 mM with ferrocene to calibrate the potentials. DMF, Pt working electrode, Pt pseudo reference electrode,  $TBAPF_6 = 150$  mM,  $v = 0.1$  V.s<sup>-1</sup>, (insert:  $I_p$  vs. C)

Further studies involving changing the scan rate (Figure S9) provided a good linear plot of  $I_p$  vs.  $v^{1/2}$ , again consistent with  $H_4L$  displaying no abnormal properties.



**S9:** Cyclic voltammograms of  $H_4L$  (5 mM) for different scan rates :0.01, 0.05, 0.1, 0.2, 0.5 and 1  $V.s^{-1}$ . Pt working electrode,  $TBAPF_6 = 150$  mM (Insert:  $I_p$  vs.  $v^{1/2}$ )

Hence, some interesting information can be reached considering Figures S8 and S10.



**S10:** A)  $H_4L$  (thick line) and  $H_2L'$  (thin line) 1 mM,  $v = 0.02$   $V.s^{-1}$ .

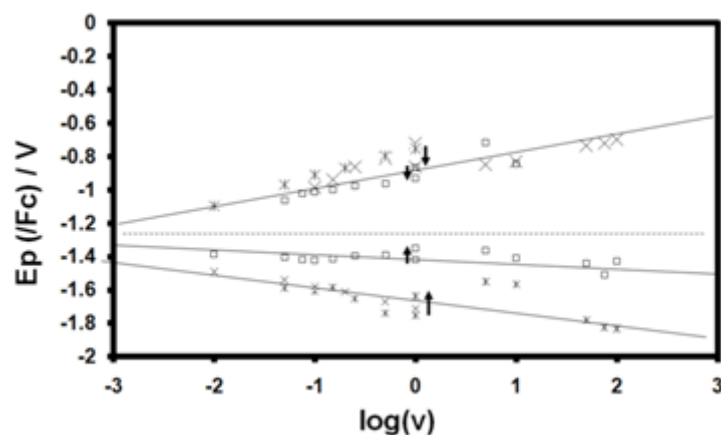
B)  $H_4L$  1 mM (thick line) and  $H_4L$  1 mM with  $HCl$  1 mM (thin line),  $v = 0.1$   $V.s^{-1}$

Pt working electrode,  $TBAPF_6 = 150$  mM, the potential of ferrocene is arbitrary fixed to 0 V.



The current intensity peaks related to  $H_4L$  and  $H_2L'$  are similar and in comparison with an equivalent of HCl, it becomes possible to indicate that this signal would correspond to only one proton. From this result, it is possible to assume that, despite of the presence of two equivalents phenol functions on  $H_4L$  molecule, statically only one is engaged. This point allows us to rule out the hypothesis (assumed previously) related to the number of active acid functions.

However,  $H_4L$  does not seem present expected evolution when the potential parameter is considered (Figures S8C and S9). This kinetic behaviour is confirmed plotting  $E_p$  vs.  $\log(v)$ . The result is presented Figure S12 and indicates that kinetic limitation has influence on the proton potential reduction in a scan rate range of  $0.002 \text{ V.s}^{-1} - 100 \text{ V.s}^{-1}$ . Hence, there is not range of scan rate wherein the potential is independent of the scan rate. In the case of compounds  $H_2L'$  and  $H_2L''$ , cyclic voltammograms (Figure S10A) and successive records show shape evolution consistent with kinetic limitations. Adsorption of ligands onto platinum electrode is probably the origin of the protons reduction kinetic limitation.



**S 12:** Plot of  $E_p$  vs.  $\log(v)$  for  $H_4L$  : 1 mM (square) and 5 mM (cross) . Arrows show measurements performed with both Pt electrode and Pt microelectrode at  $1 \text{ V.s}^{-1}$  to indicate that resistance effect is not the only limitation.

## EPR

**EPR measurement:** EPR spectra were recorded on EMX Bruker spectrometer (operating at 10 GHz) equipped with an Oxford Instruments ESR 900 continuous-flow helium cryostat. The static field was controlled with a Hall probe, whereas the microwave frequency was simultaneously recorded with a frequency counter (HP-5350 B). Samples were illuminated with an Argon-Krypton laser (model stability 2018-RM from Spectra Physic) using the multiline mode (superposition of visible lines from the blue (457 nm) up to the green (574 nm)) directly *in situ* in the EPR cavity.

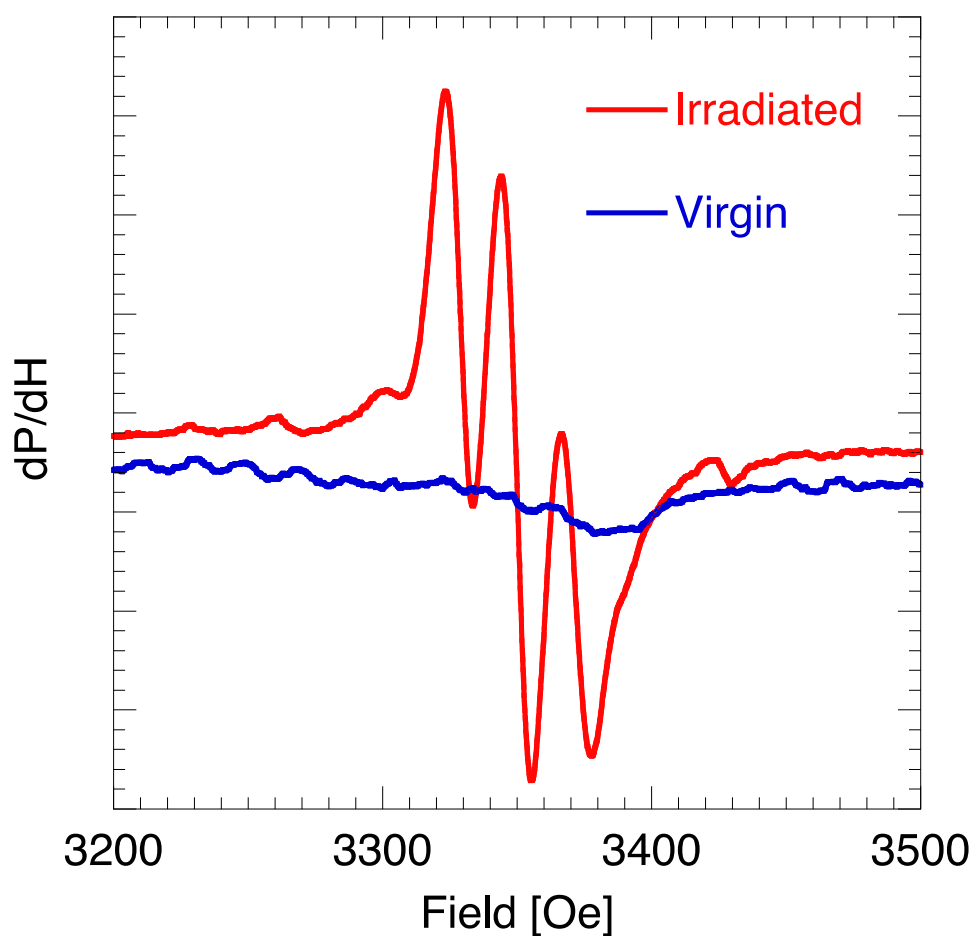
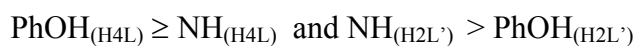


Fig S13: EPR spectra of the iron complex in DMF at 6 K: blue line before irradiation, red line after 3 hours of irradiation.

In this study, chemical physics properties comparisons have been performed between  $N,N'$ -bis(salicyl)hydrazine and related mono salicylic hydrazide derivatives. UV-Vis spectroscopy and electrochemistry studies allow us to point out acid-base differences despite apparent close chemical similarities. Although for each type of molecule, only one proton is involved in the acid-base equilibrium, the proton exchange site is different between  $N,N'$ -bis(salicyl)hydrazine and related mono salicylic hydrazide derivatives. In the first case, the Ph-OH group provides protons whereas in the second case, the NH group is engaged in the acid-base equilibrium. This observation can be understood assuming that acidic power of identical acid functions are affected because of the presence or not of the hydrazide /hydrazone combination within the molecules. Hence, a relative positioning acidic power can be proposed:



## References

- [1] N. Bouslimani, N. Clément, G. Rogez, P. Turek, S. Choua, S. Dagorne, R. Welter, *Inorganica Chimica Acta* 2010, **363**, 213–220.
- [2] R. M. Issa, Y. M. Temerk, M. M. Ghoneim, J. Y. Maghrabi, *Bull. Fac. Sci. K.A.U. Jeddah* 1978, **2**, 167-178.
- [3] H. F. F. El-Baradie, M. A. Khattab, R. M. Issa, J. Y. Maghrabi, *J. Chem. Tech. Biotechnol.* 1983, **33A**, 123-129.
- [4] E. Anxolabéhère-Mallart, C. Costentin, C. Policar, M. Robert, J.-M. Savéant, A.-L. Teillout, *Faraday Discuss.* 2011, **148**, 83-95.
- [5] S. S. Kurek, B.J. Laskowka, A. Stoklosa, *Electrochim. Acta*, 2006, **51**, 2606-2414.